Electronic Supplementary Material (ESI) for Inorganic Chemistry Frontiers.

Supporting Information

Free-Standing $Li_{1.2}Mn_{0.54}Ni_{0.13}Co_{0.13}O_2$/MWCNTs Framework for High-Energy Lithium Ion Batteries

Congjie Lv, Yi Peng, Jing Yang, Chen Liu, Xiaochuan Duan, Jianmin Ma, and Taihong Wang**

S1. Results and Discussion

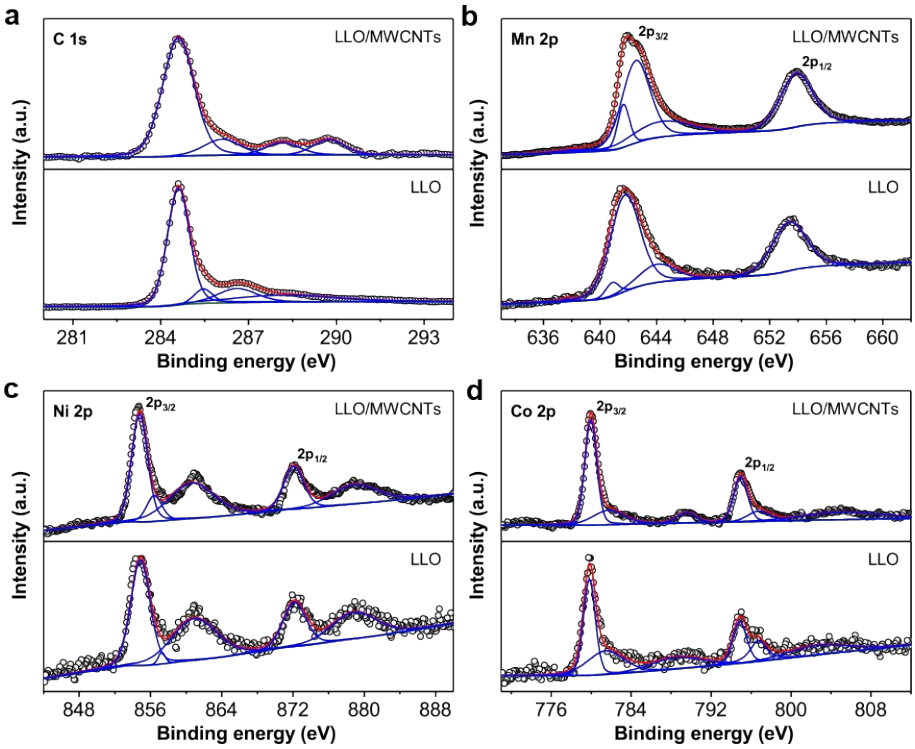

Figure S1. High resolution XPS spectrum of (a) C 1s, (b) Mn 2p, (c) Ni 2p and (d) Co 2p for the LLO/MWCNTs and LLO.

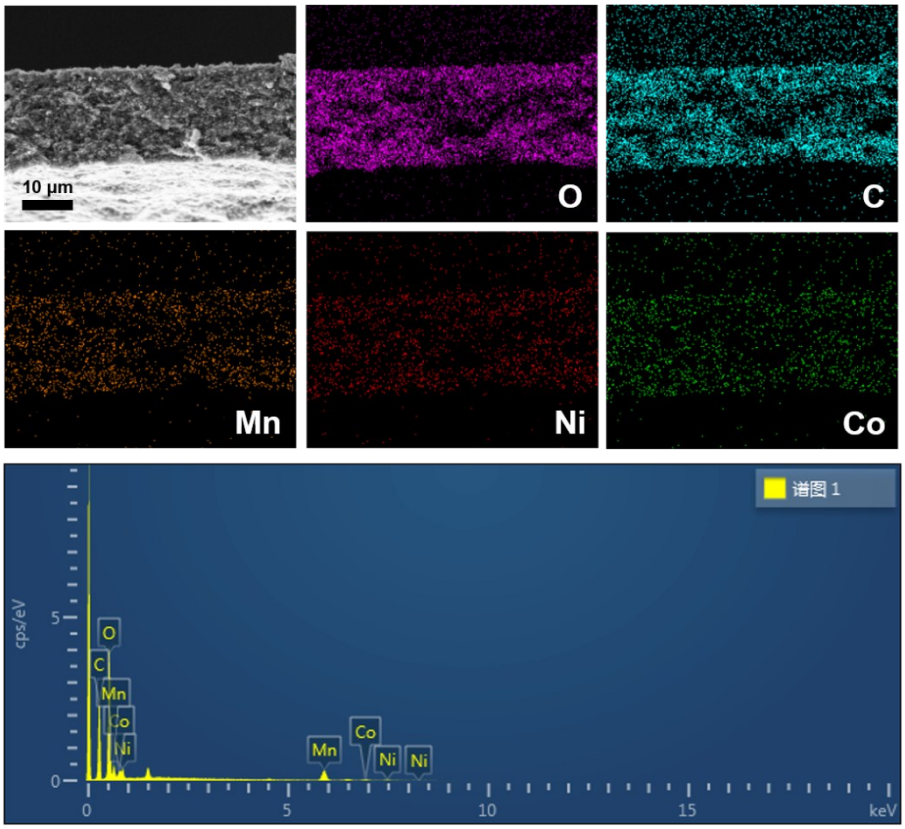

Figure S2. Elemental mappings and the corresponding EDX analysis of the LLO/MWCNTs.

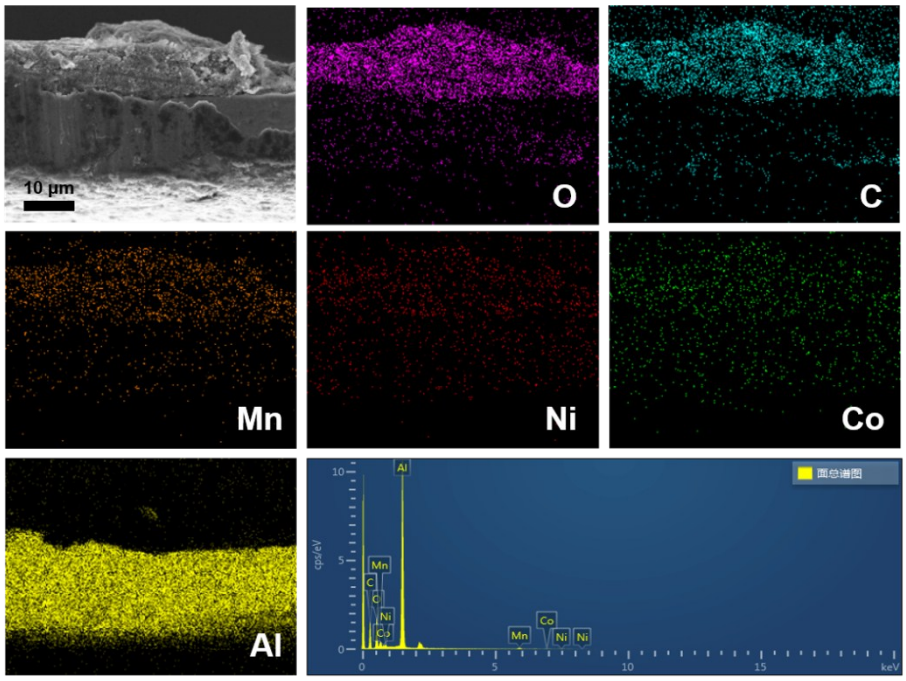

Figure S3. Elemental mappings and the corresponding EDX analysis of the LLO.

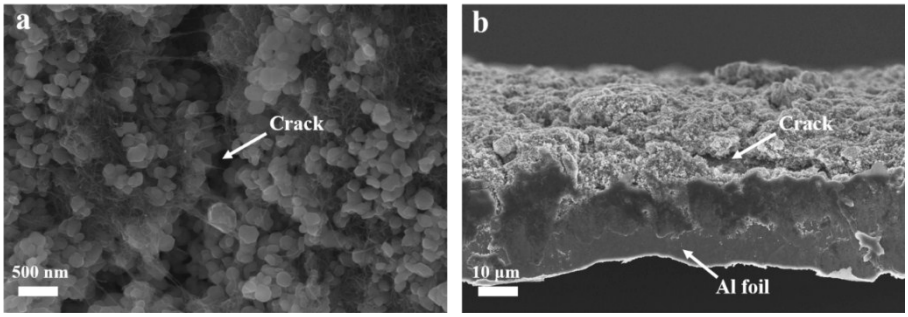

Figure S4. (a) Top-viewed and (b) cross-sectional SEM images of electrode prepared by a slurry coating method in which the MWCNTs were used as conductive additives.

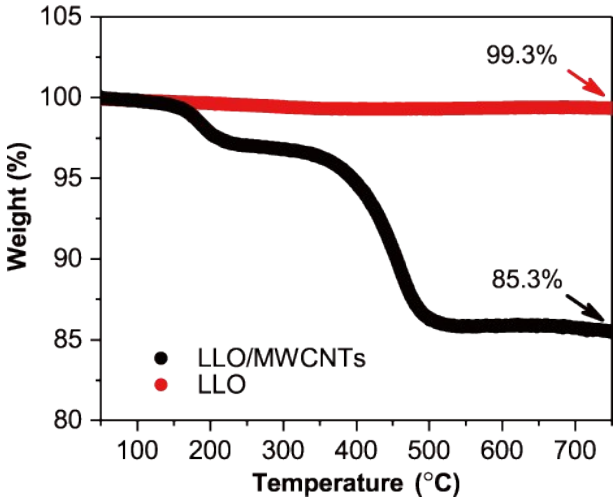

Figure S5. TG curves of the LLO/MWCNTs.

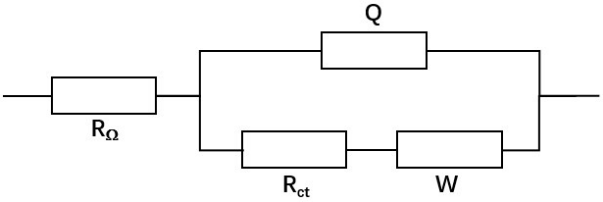

Figure S6. The simplified equivalent circuit of the LLO/MWCNTs and LLO.

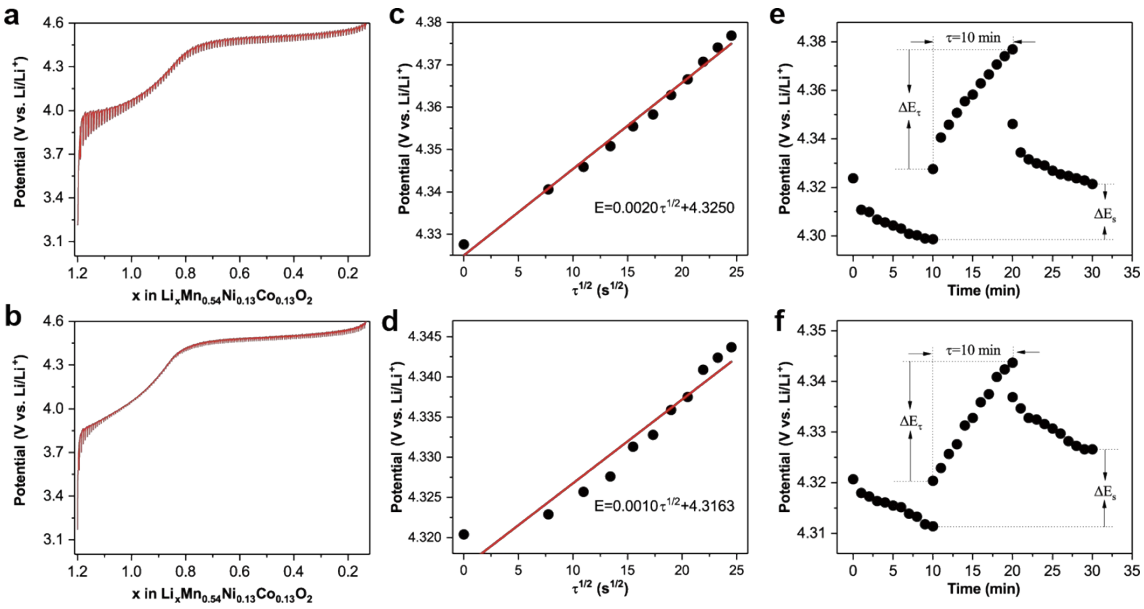

Figure S7. GITT curves of (a) LLO/MWCNTs and (b) LLO cells in the initial charge up to 4.6 V. Linear behavior of E vs. $\tau^{1/2}$ of (c) LLO/MWCNTs and (d) LLO cells. t vs. E profiles for a single GITT titration of (e) LLO/MWCNTs and (f) LLO cells.

To evaluate the Li diffusion constant in a half cell configuration, galvanostatic intermittent titration technique (GITT) was carried out. Figure S7 (a) and (b) shows the GITT curves of LLO/MWCNTs and LLO cells during the initial charge process up to 4.6 V. The Li^+ ions diffusion coefficients can be calculated from the formula:

$$D_{Li+} = \frac{4}{\pi\tau}\left(\frac{mV_M}{MA}\right)^2\left(\frac{\Delta E_s}{\tau(dE_\tau/d\sqrt{\tau})}\right)^2 \quad (\tau \le \frac{L^2}{D_{Li+}})$$

Where V_M is the molar volume of the compound, which is 20.06 cm^3 mol^{-1}, m and M are the mass and molecular weight of active material, respectively. A is the active surface area of the electrode. When E versus $\tau^{1/2}$ shows a straight line behavior over entire time period of current flux shown in Figure S7 (c) and (d), the above formula can be further simplified as:

$$D_{Li+} = \frac{4}{\pi\tau}\left(\frac{mV_M}{MA}\right)^2\left(\frac{\Delta E_s}{\Delta E_\tau}\right)^2$$

Figure S7 (e) and (f) show the t vs. E profiles for a single titration of LLO/MWCNTs and LLO cells. Based on the GITT measurement and the above formula, the diffusion coefficients of Li^+ ions at can be obtained. At the charge process below 4.5 V, the Li^+ ions extract from the $LiMO_2$ component. The D_{Li} are about 1.25×10^{-12} cm^2 s^{-1} and 2.70×10^{-13} cm^2 s^{-1} for LLO/MWCNTs and LLO electrodes, respectively. Afterwards, at the platform (approximately 4.55 V), the D_{Li} are about 5.00×10^{-14} cm^2 s^{-1} and 1.08×10^{-14} cm^2 s^{-1} for LLO/MWCNTs and LLO electrodes, respectively. It probably indicates that the diffusion of Li^+ in Li_2MnO_3 component is slower than that in $LiMO_2$ component. The calculated Li^+ ions diffusion coefficient of LLO/MWCNTs cell is larger than that of LLO cell indicating that faster Li^+ ion insertion/extraction kinetics for LLO/MWCNTs cell.

Table S1. The fitting values of the resistance components in the simplified equivalent circuit.

Components	R_{Ω}/Ω	R_{ct}/Ω	R_{total}/Ω
LLO/MWCNTs	2.61	42.48	45.09
LLO	3.06	88.64	91.70

Table S2. The sheet resistances and conductivities of LLO/MWCNTs and LLO electrodes.

Electrodes	$R_{\square 1}/(\Omega/\square)$	$R_{\square 2}/(\Omega/\square)$	$R_{\square 3}/(\Omega/\square)$	$R_{\square avg}/(\Omega/\square)$	σ/(S/cm)
LLO/MWCNTs	5.97	6.71	4.83	5.84	85.62
LLO	11.88	13.71	10.11	11.90	33.61

Table S3. Comparison of the electrochemical performance of LLO/MWCNTs in this work with that of LLO in the literature.

Ref	Structure	Synthesis	Voltage	Initial discharge capacity (mAh g^{-1})	Initial coulombic efficiency	Capicity (mAh g^{-1})	Cycling performance/Capacity retention
1	Hollow spherical $Li_{1.2}Ni_{0.13}Co_{0.13}Mn_{0.54}O_2$ (2-3 μm)	Sacrificing template method	2.0-4.8 V	268.7 (0.1 C)	83.7%	184.2 (1 C)	174.5 mAh g^{-1} (200 th)/94.7%
						165.7 (2 C)	—
						138.1 (5 C)	—
2	Spherical $Li_{1.2}Ni_{0.13}Co_{0.13}Mn_{0.54}O_2$ (~10 μm)	A combination of ballmilling, spray drying and a solid-state synthesis	2.0-4.8 V	287.8 (0.1 C)	85%	~210 (1 C)	~175 mAh g^{-1} (200 th)/83.3%
3	$Li_{1.2}Mn_{0.54}Ni_{0.13}Co_{0.13}Si_{0.03}O_2$ particles (~200 nm)	Sol-gel method	2.0-4.8 V	286.5 (0.1 C)	81.41%	210.5 (1 C)	~160 mAh g^{-1} (100 th)/70.4%
						173.6 (2 C)	—
						50 (10 C)	—

	$Li_{1.2}Mn_{0.54}Ni_{0.13}Co_{0.13}Sn_{0.03}O_2$ particles (~200 nm)			279.3 (0.1 C)	82.13%	198.9 (1 C)	~185 mAh g^{-1} (100 th)/86.2%
						177.5 (2 C)	—
						127.1 (10 C)	—
4	Spherical $Li_{1.2}Ni_{0.13}Co_{0.13}Mn_{0.54}O_2$@$Li_3PO_4$/C (10-15 μm)	Co-precipitation method	2.0-4.6 V	~266 (0.1 C)	88.3%	218.3 (1 C)	190.5 mAh g^{-1} (200 th)/87.3%
5	Spherical $Li_{1.2-x}Na_xNi_{0.13}Co_{0.13}Mn_{0.54}O_2$ (10-30 μm)	Co-precipitation method	2.0-4.7 V	286 (0.1 C)	87%	215 (1 C)	—
						185 (2 C)	—
6	Carbon coated $Li_{1.2}Ni_{0.13}Co_{0.13}Mn_{0.54}O_2$ particles (100-200 nm)	Hydrothermal approach	2.0-4.8 V	264 (0.2 C)	96.4%	264 (0.2 C)	~182 mAh g^{-1} (100 th)/68.9%
						100 (10 C)	70 mAh g^{-1} (100 th)/70%
7	Spherical Al_2O_3 coated $Li_{1.2}Ni_{0.13}Co_{0.13}Mn_{0.54}O_2$ (2-3 μm)	Spray pyrolysis process	2.0-4.8 V	248 (0.1 C)	84.1%	—	—
			2.0-4.6 V	—	—	~190 (C/3)	~155 mAh g^{-1} (50 th)/81.6%
	Spherical TiO_2 coated $Li_{1.2}Ni_{0.13}Mn_{0.54}Co_{0.13}O_2$ (2-3 μm)		2.0-4.8 V	287 (0.1 C)	87.6%	—	—
			2.0-4.6 V	—	—	~230 (C/3)	~175 mAh g^{-1} (50 th)/76.1%
8	Graphene wrapped $Li_{1.2}Ni_{0.13}Co_{0.13}Mn_{0.54}O_2$ nanoparticles (200-300 nm)	Sol-gel method	2.0-4.7 V	290 (0.05 C)	74%	~250 (0.1 C)	—
						~188 (0.5 C)	~162 (100 th) 86.2%
						~150 (1 C)	—
This Work	**MWCNTs wrapped $Li_{1.2}Mn_{0.54}Ni_{0.13}Co_{0.13}O_2$**	**Hydrothermal method followed by**	**2.0-4.8 V**	**318.2 (0.1 C)**	**91.1%**	**218.1 (1 C)**	**209.2 mAh g^{-1} (200 th) 95.9%**
						207.7 (2 C)	**191.2 mAh g^{-1} (200 th) 92.1%**

	(width of 150-300 nm and thickness of 80-150 nm)	**filtration**				**185.7 (5 C)**	**175.6 mAh g^{-1} (200 th) 94.6%**
						144.2 (10 C)	**121.6 mAh g^{-1} (500 th) 84.3%**

References

1. W. Ding, X. Cui, J. Lei, X. Lin, S. Zhao, Q.-H. Wu, M. Zheng and Q. Dong, *Electrochimica Acta*, 2018, **264**, 260-268.
2. Z. Wang, Y. Yin, Y. Ren, Z. Wang, M. Gao, T. Ma, W. Zhuang, S. Lu, A. Fan, K. Amine and Z. Chen, *Nano Energy*, 2017, **31**, 247-257.
3. Z. Ding, M. Xu, J. Liu, Q. Huang, L. Chen, P. Wang, D. G. Ivey and W. Wei, *ACS Appl Mater Interfaces*, 2017, **9**, 20519-20526.
4. H. Liu, C. Chen, C. Du, X. He, G. Yin, B. Song, P. Zuo, X. Cheng, Y. Ma and Y. Gao, *Journal of Materials Chemistry A*, 2015, **3**, 2634-2641.
5. R.-P. Qing, J.-L. Shi, D.-D. Xiao, X.-D. Zhang, Y.-X. Yin, Y.-B. Zhai, L. Gu and Y.-G. Guo, *Advanced Energy Materials*, 2016, **6**.
6. B. Song, C. Zhou, Y. Chen, Z. Liu, M. O. Lai, J. Xue and L. Lu, *RSC Adv.*, 2014, **4**, 44244-44252.
7. X. Zhang, I. Belharouak, L. Li, Y. Lei, J. W. Elam, A. Nie, X. Chen, R. S. Yassar and R. L. Axelbaum, *Advanced Energy Materials*, 2013, **3**, 1299-1307.
8. K. C. Jiang, X. L. Wu, Y. X. Yin, J. S. Lee, J. Kim and Y. G. Guo, *ACS Appl Mater Interfaces*, 2012, **4**, 4858-4863.